possesses terminal Nb=O sites on the surface, and the number of terminal Nb=O sites can be eliminated by high-temperature calcinations which dramatically decreased the surface area. The in situ Raman studies confirm the presence of the terminal Nb=O surface sites on amorphous $Nb_2O_5 \cdot nH_2O$ and the assignment of the Raman band at ~900 cm^{-1} to the terminal Nb=O surface sites.

Conclusions

The relationships between niobium oxide structures and their corresponding Raman spectra were systematically studied for various types of niobium oxide compounds. The Raman frequencies strongly depend on the bond order of the niobium oxide structure. A higher niobium–oxygen bond order, corresponding to a shorter bond distance, shifts the Raman frequency to higher wavenumbers. Most of the niobium oxide compounds possess an octahedrally coordinated NbO_6 structure, slightly or highly distorted. Only a few niobium oxide compounds (such as $YNbO_4$, $YbNbO_4$, $LaNbO_4$, and $SmNbO_4$) can possess a tetrahedrally coordinated NbO_4 structure that is similar to the scheelite-like structure. For the tetrahedral NbO_4 structure, the major Raman frequency appears in the 790–830-cm^{-1} region. For the slightly distorted octahedral NbO_6 structure, the major Raman frequencies appear in the 500–700-cm^{-1} wavenumber region. For the highly distorted octahedral NbO_6 structure, the Raman frequency shifts from the 500–700- to the 850–1000-cm^{-1} region. Both slightly distorted and highly distorted octahedral NbO_6 sites coexist in the $KCa_2Na_{n-3}Nb_nO_{3n+1}$, n = 3–5, layered compounds. The distortions in the niobium oxide compounds are caused by the formation of corner- or edge-shared NbO_6 octahedra.

Acknowledgment. Financial support for this work by Niobium Products Company Inc. is gratefully acknowledged. We wish to thank A. Jacobson of Exxon Research and Engineering Co. for providing the layered niobium oxide compounds and S. Yoshida of Kyoto University, Japan, for providing the $YbNbO_4$ compound.

Registry No. $KNbO_3$, 12030-85-2; $NaNbO_3$, 12034-09-2; $LiNbO_3$, 12031-63-9; $K_8Nb_6O_{19}$, 12031-11-7; $AlNbO_4$, 12258-25-2; $Nb(CH_2O_4)_5$, 12404-95-4; $K(Ca_2Na_2)Nb_5O_{16}$, 98820-43-0; $K(Ca_2Na)Nb_4O_{13}$, 98820-40-7; $KCA_2Nb_3O_{10}$, 80487-87-2; $HCa_2Nb_3O_{10}$, 98820-36-1; Nb_2O_5, 1313-96-8; $Nb_2O_5 \cdot nH_2O$, 12326-08-8; $YbNbO_4$, 12034-62-7.

Phase-Transfer Palladium(0)-Catalyzed Polymerization Reactions. 6. Synthesis and Thermotropic Behavior of Mono- and Difluorinated 1,2-Bis(4-*n*-alkoxyphenyl)acetylene Monomers†

Coleen Pugh and Virgil Percec*

Department of Macromolecular Science, Case Western Reserve University, Cleveland, Ohio 44106

Received May 30, 1990

Symmetrically difluorinated 1,2-bis(3-fluoro-4-*n*-alkoxyphenyl)acetylene (n = 4–12) and asymmetric, monofluorinated 1-(3-fluoro-4-*n*-alkoxyphenyl)-2-(4-*n*-alkoxyphenyl)acetylene (n = 5–12) monomers were prepared by a one-pot, phase-transfer Pd(0)/Cu(I)-catalyzed three-step coupling of the appropriate aryl halides with 2-methyl-3-butyn-2-ol. All odd members of the 1,2-bis(3-fluoro-4-*n*-alkoxyphenyl)acetylene series are crystalline with a virtual nematic mesophase. All even members of the series present monotropic nematic mesophases. The thermotropic behavior of the 1-(3-fluoro-4-*n*-alkoxyphenyl)-2-(4-*n*-alkoxyphenyl)acetylenes changes continuously with n. The n = 5 derivative is crystalline. The n = 6–10 derivatives each have an enantiotropic nematic mesophase. In addition, the n = 7, 8 derivatives exhibit an enantiotropic smectic mesophase, and the n = 9, 10 derivatives exhibit monotropic smectic C mesophases. Both the nematic and smectic C mesophases of the n = 11, 12 derivatives are monotropic.

Introduction

In a recent publication,[1] we described a one pot, solid–liquid phase-transfer Pd(0)/Cu(I)-catalyzed synthesis of 1,2-bis(4-alkoxyaryl)acetylenes from aryl halides deactivated by alkoxy substituents. The three-step, one-pot synthesis outlined in Scheme I was adapted from Carpita[2] et al.'s liquid–liquid phase-transfer catalyzed synthesis of diheteroarylacetylenes. In the first step, an aromatic halide is coupled with a monoprotected acetylene. The resulting carbinol derivative is deprotected in the second step with formation of an aryl acetylene, which is then coupled with a second aryl halide in the final step. In this phase-transfer catalyzed (PTC), one-pot procedure, only the final diarylacetylene product is isolated.

The subsequent papers in this series described the thermotropic behavior of both symmetrically and asymmetrically substituted 1,2-bis(4-alkoxyaryl)acetylene monomers.[3-5] The linear 1,2-bis(4-*n*-alkoxyphenyl)acetylenes

† Part 5: Pugh, C.; Tarnstrom, C.; Percec, V. *Mol. Cryst. Liq. Cryst.*, in press.

* To whom correspondence should be sent.

(1) Pugh, C.; Percec, V. *J. Polym. Sci., Polym. Chem. Ed.* **1990**, *28*, 1101.
(2) Carpita, A.; Lessi, A.; Rossi, R. *Synthesis* **1984**, 571.
(3) Pugh, C.; Percec, V. *Mol. Cryst. Liq. Cryst.* **1990**, *178*, 193.
(4) Pugh, C.; Percec, V. *Polym. Bull.* **1990**, *23*, 177.
(5) Pugh, C.; Tarnstrom, C.; Percec, V. *Mol. Cryst. Liq. Cryst.*, in press.

0897-4756/91/2803-0107$02.50/0

Scheme I. One-Pot, Three-Step, Phase-Transfer Pd(0)/Cu(I)-Catalyzed Synthesis of 1,2-Diarylacetylenes

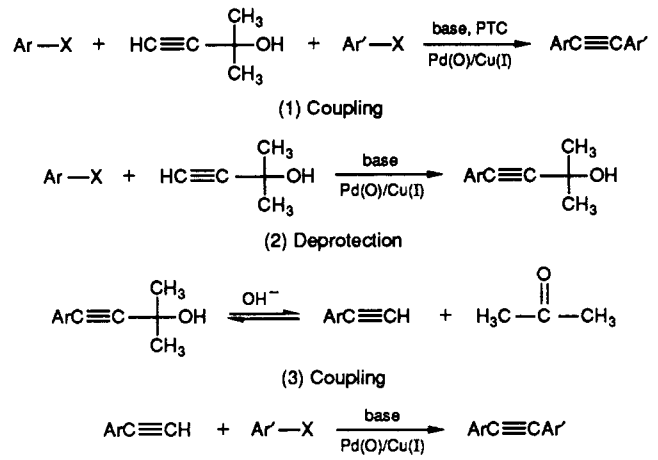

can be divided into three groups.[3] The lower homologues with n = 3 are crystalline. Those with n = 4–8 present crystalline and crystalline/smectic polymorphism in addition to a nematic mesophase. The higher homologues with n = 10–12 display an enantiotropic smectic C (s_C) phase directly below the nematic mesophase. Upon further cooling, the higher homologues with n = 9–12 also exhibit an additional monotropic smectic mesophase, possibly smectic B, before crystallizing.

In addition to the symmtrically substituted, linear 1,2-bis(4-n-alkoxyphenyl)acetylenes, diarylacetylenes with both symmetric and asymmetric methyl branching in either the alkoxy substituents or in the aromatic ring(s) of the mesogen were examined.[3-5] In general, both symmetry and methyl branching destabilize liquid crystallinity more than crystallinity, such that only the asymmetrically branched derivatives display a nematic mesophase in addition to melting/crystallization. However, if the mesogen is extended by one phenylethynyl unit, an enantiotropic nematic mesophase is also realized in the symmetrically branched derivatives.[4] Chiral methyl-branched 1-(4-n-alkoxyphenyl)-2-(4-[S(−)-(2-methylbutyl)oxy]phenyl)-acetylenes were also prepared.[5] Those with n = 8–10 present enantiotropic cholesteric mesophases, and those with n = 11, 12 present monotropic cholesteric mesophases.

One of the more unusual characteristics of these 1,2-bis(4-n-alkoxyphenyl)acetylenes is the existence in the higher homologues of the enantiotropic s_C mesophase directly below the nematic mesophase. In addition to being a common feature of dialkoxy compounds with long side chains,[6,7] s_C mesophases are also often exhibited by laterally fluorinated terphenyls,[7-9] fluorinated phenylbiphenyl carboxylates,[10] 2,3-difluorinated biphenyls,[11] 2,3-difluorinated phenyl benzoates,[7] 2,3-difluorinated phenylbiphenyl carboxylates,[7] and 2,3-difluorinated phenylbicyclohexyl carboxylates.[7] As explained by Gray,[12] lateral substituents usually exert two opposing effects. That is, while the change in the molecular polarizability may increase the mesophase thermal stability, the decrease in the length/breadth ratio causes a decrease. The latter effect usually dominates.[12] Because of their small size, lateral fluorine substituents are used to minimize the destabilizing effect on the mesophase. Fluorinated liquid crystals are also of tremendous interest because of the tendency of the fluorine substituent(s) to transfer s_A into s_C mesophases,[7,11] to suppress and eliminate more ordered smectic mesophases,[7,9-12] and to decrease the positive dielectric anisotropy ($\Delta_\epsilon = \epsilon_\parallel - \epsilon_\perp$).[7,10,11] The dielectric anisotropy becomes more negative as the number of fluorine substituents in the molecule increases, with 2,3-difluorination being especially effective.[7,10,11]

In our continuing efforts at determining the effects of structural variations on the thermotropic behavior of 1,2-bis(4-dialkoxyaryl)acetylenes, this paper presents the synthesis and characterization of asymmetric, monofluorinated 1-(3-fluoro-4-n-alkoxyphenyl)-2-(4-n-alkoxyphenyl)acetylene and of symmetrically difluorinated 1,2-bis(3-fluoro-4-n-alkoxyphenyl)acetylene monomers.

Experimental Section

Materials. 4-Iodophenol (99%), bis(triphenylphosphine)-palladium(II) chloride (99%), 4-bromo-2-fluorophenol (98%), tetrabutylammonium hydrogen sulfate (TBAH, 97%), and triphenylphosphine (99%) were used as received from Aldrich. Cuprous iodide (Alfa, 98%) and 2-methyl-3-butyn-2-ol (Fluka, 99%) were also used as received. Triethylamine (Fisher, reagent) was distilled under argon from KOH. Tetrahydrofuran (THF, distilled from $LiAlH_4$) was deaerated before each use by bubbling argon through the solvent for at least 30 min.

Techniques. ^{1}H NMR (200 MHz, spectra δ, ppm) were recorded on a Varian XL-200 spectrometer. All spectra were recorded in $CDCl_3$ with TMS as the internal standard.

Purity was determined by high-pressure liquid chromatography/gel permeation chromatography (HPLC/GPC) with a Perkin-Elmer Series 10 LC instrument equipped with an LC-100 column oven (40 °C), an LC-600 autosampler, and a Nelson Analytical 900 Series data station. Measurements were made using a UV detector after ^{1}H NMR spectroscopy demonstrated that non-UV-absorbing impurities were absent, with $CHCl_3$ as solvent and a 100-Å PL gel column (0.9 or 1.0 mL/min).

A Perkin-Elmer DSC-4 differential scanning calorimeter equipped with a TADS 3600 data station was used to determine the thermal transitions, which were read as the maximum or minimum of the endothermic or exothermic peaks. All heating and cooling rates were 10 °C/min. Tabulated thermal transitions were read from reproducible second or later heating scans and first or later cooling scans. Both enthalpy changes and transition temperatures were determined by using indium as a calibration standard.

A Carl-Zeiss optical polarized microscope (magnification 100×) equipped with a Mettler FP 82 hot stage and a Mettle FP 800 central processor was used to observe the thermal transitions and to analyze the anisotropic textures.[13,14]

Etherification of 4-Bromo-2-fluorophenol and 4-Iodophenol. The etherification of 4-bromo-2-fluorophenol and of 4-iodophenol with n-bromoalkanes followed the procedures used to etherify 4-bromophenol.[1] All resulting compounds were >99.1% pure.

1-Bromo-3-fluoro-4-n-alkoxybenzenes (49–82% yield): All 1-bromo-3-fluoro-4-n-alkoxybenzenes have identical ^{1}H NMR chemical shifts: δ 0.8 (t, CH_3) 1.0–1.5 (m, $[CH_2]_{n-3}$), 1.8 (m, OCH_2CH_2), 4.0 (t, OCH_2), 6.8 (t, 1 aromatic proton ortho to OR), 7.2 (t, 2 aromatic protons ortho to Br).

1-Iodo-4-n-alkoxybenzenes (53–86% yield): all 1-iodo-4-n-alkoxybenzenes have identical ^{1}H NMR chemical shifts: δ 0.9

(6) Demus, D.; Zaschke, H. *Flussige Kristalle in Tabellen II*; VEB Deutscher Verlag fur Grundstoffindustrie: Liepzig, 1984.
(7) Reiffenrath, V.; Krause, J.; Plach, H. F.; Weber, G. *Liq. Cryst.* **1989**, *5*, 159.
(8) Chan, L. K. M.; Gray, G. W.; Lacey, D.; Toyne, K. J. *Mol. Cryst. Liq. Cryst.* **1988**, *158B*, 209.
(9) Chan, L. K. M.; Gray, G. W.; Lacey, D. *Mol. Cryst. Liq. Cryst.* **1985**, *123*, 185.
(10) Chambers, M.; Clemitson, R.; Coates, D.; Greenfield, S.; Jenner, J. A.; Sage, I. C. *Liq. Cryst.* **1989**, *5*. 153.
(11) Gray, G. W.; Hird, M.; Lacey, D.; Toyne, K. J. *J. Chem. Soc., Perkin Trans.* **2 1989**, 2041.
(12) Gray, G. W.; Hogg, C.; Lacey, D. *Mol. Cryst. Liq. Cryst.* **1981**, *67*, 1.
(13) Demus, D.; Richter, L. *Textures of Liquid Crystals*; Verlag Chemie: Weinheim, 1978.
(14) Gray, G. W.; Goodby, J. W. *Smectic Liquid Crystals, Textures and Structures*; Leonard Hill: Glasgow, 1984.

Table I. Synthesis of Symmetric 1,2-Bis(3-difluoro-4-*n*-alkoxyphenyl)acetylenes[a]

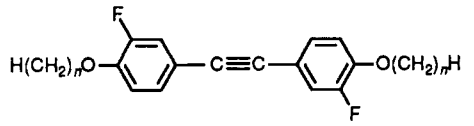

n	ArX, mmol	Pd, mol %	mol of CuI/ mol of Pd	mol of PPh_3/ mol of Pd	reaction time, h: before KOH addn	reaction time, h: after KOH addn	% yield	(% yield)$^{1/3}$
4	7.7	2.7	3.6	5.2	7	40	35	70
5	7.3	2.6	3.7	5.3	8	43	25	63
6	8.0	2.6	3.7	5.3	12	28	46	77
7	7.0	2.5	3.8	5.3	6	43	37	72
8[b]	6.6	2.6	3.7	5.3	12	37	61	85
9	6.4	2.6	3.6	5.3	6	44	39	73
10	7.5	1.7	4.6	6.4	12	37	48	78
11	7.3	2.6	3.7	5.3	6	40	62	85
12	7.0	2.6	3.7	5.3	8	37	48	78

[a] ArX = 1-bromo-3-fluoro-(4-*n*-alkoxy)benzene. Reaction conditions: 1.0–1.3 mL of THF and 0.53–0.57 mmol of 2-methyl-3-butyn-2-ol per mmol of ArX; 2 mol of NEt_2, 3 mol of KOH, and 15–20 mol % TBAH per mol of 2-methyl-3-butyn-2-ol. [b] 0.68 mmol of 2-methyl-3-butyn-2-ol vs 1 mmol of ArX.

(5, CH_3), 1.0–1.6 (m, $[CH_2]_{n-3}$), 1.7 (m, OCH_2CH_2), 3.9 (t, OCH_2), 6.6 (d, 2 aromatic protons ortho to OR), 7.5 (d, 2 aromatic protons ortho to I).

Phase Transfer Pd(0)/Cu(I)-Catalyzed Acetylene Coupling Reactions. With the exception of 1,2-bis[3-fluoro-4-(*n*-nonyloxy)phenyl]acetylene (98.6% pure), the purity of all compounds resulting from the following coupling and purification procedures is at least 99.0%.

(1) Synthesis of 1,2-Bis(3-fluoro-4-*n*-alkoxyphenyl)-acetylenes. In a typical procedure, a solution of 2-methyl-3-butyn-2-ol (0.34 g, 4.0 mmol), triethylamine (0.82 g, 8.1 mmol) and 1-bromo-3-fluoro-4-(*n*-undecyloxy)benzene (2.5 g, 7.3 mmol) in deaerated THF (8 mL) was added via an addition funnel to a mixture of cuprous iodide (0.13 g, 0.70 mmol), triphenylphosphine (0.27 g, 1.0 mmol) and $PdCl_2(PPh_3)_2$ (0.13 g, 0.19 mmol) in a round-bottom flask equipped with a reflux condenser connected to an argon inlet/outlet. The reaction mixture was heated to reflux for 6 h. An intimately ground mixture of TBAH (0.28 g, 0.83 mmol) and KOH (0.71 g, 13 mmol) was then added. After refluxing 40 h, the reaction mixture was allowed to cool to room temperature, and a saturated aqueous solution of ammonium chloride (130 mL) was added. This was stirred 1 h and then extracted five times with toluene, leaving a very blue aqueous phase. The toluene extracts were dried over $MgSO_4$. The filtered and condensed product was purified by column chromatography on silica gel using hexane as eluent. Recrystallization from ethanol (130 mL) yielded 1.3 g (62%) of 1,2-bis[3-fluoro-4-(*n*-undecyloxy)phenyl]acetylene, purity >99.9%.

The results of the synthesis of the 1,2-bis(3-fluoro-4-*n*-alkoxyphenyl)acetylenes (n = 4–12) are presented in Table I. Their ^{1}H NMR chemical shifts are identical: δ 0.85 (t, CH_3, 6 protons), 1.0–1.6 (m, $[CH_2]_{n-3}$, 4[n – 3] protons), 1.8 (m, OCH_2CH_2, 4 protons), 4.0 (t, OCH_2, 4 protons), 6.9 (t, 2 aromatic protons ortho to OR), 7.2 (d, 4 aromatic protons ortho to C≡C).

(2) Synthesis of 1-(3-Fluoro-4-*n*-alkoxyphenyl)-2-(4-*n*-alkoxyphenyl)acetylenes. In a typical procedure, a solution of 2-methyl-3-butyn-2-ol (0.29 g, 3.4 mmol), triethylamine (0.67 g, 6.7 mmol), and 1-iodo-4-(*n*-heptyloxy)benzene (1.0 g, 3.1 mmol) in deaerated THF (4 mL) was added via an addition funnel to a mixture of cuprous iodide (0.091 g, 0.48 mmol), triphenylphosphine (0.18 g, 0.86 mmol), and $PdCl_2(PPh_3)_2$ (0.089 g, 0.13 mmol) in a round-bottom flask equipped with a reflux condenser connected to an argon inlet/outlet. The reaction mixture was heated to reflux for 6 h. ^{1}H NMR spectroscopy demonstrated that only a trace of aryl iodide was unreacted after 2.5 h. 1-Bromo-3-fluoro-4-(*n*-heptyloxy)benzene (0.91 g, 3.2 mmol) in deaerated THF (2 mL) and an intimately ground mixture of TBAH (0.24 g, 0.69 mmol) and KOH (0.52 g, 9.4 mmol) were then successively added. After refluxing for 46 h, the reaction mixture was allowed to cool to room temperature, and a saturated aqueous solution of ammonium chloride (100 mL) was added. This was stirred 1 h and then extracted six times with toluene, leaving a light blue aqueous phase. The toluene extracts were dried over $MgSO_4$. The filtered and condensed product was purified by column chromatography on silica gel using hexane as eluent. Recrystallization from ethanol (50 mL) yielded 0.28 g (21%) of 1-[3-fluoro-4-(*n*-heptyloxy)phenyl]-2-[4-(*n*-heptyloxy)phenyl]-acetylene, purity 99.4%. The results of the acetylene coupling reactions using this procedure (method C of ref 1) are presented in Table II. The ^{1}H NMR chemical shifts of the 1-(3-fluoro-4-*n*-alkoxyphenyl)-2-(4′-*n*-alkoxyphenyl)acetylenes (n = 5–12) are identical: δ 0.8 (t, CH_3, 6 protons), 1.0–1.6 (m, $[CH_2]_{n-3}$, 4[n – 3] protons), 1.8 (m, OCH_2CH_2, 4 protons), 4.0 (m, OCH_2, 4 protons), 6.8 (t, 3 aromatic protons ortho to OR), 7.2 (d, 2 aromatic protons ortho to C≡C and ortho or meta to F), 7.4 (d, 2 aromatic protons ortho to C≡C and meta to OR).

Table II. Synthesis of Asymmetric 1-(3-Fluoro-4-*n*-alkoxyphenyl)-2-(4-*n*-alkoxyphenyl)-acetylenes[a]

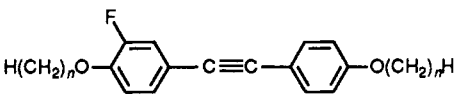

n	Ar^1X, mmol	reaction time, h: before KOH addn	reaction time, h: after KOH addn	% yield	(% yield)$^{1/3}$
5	6.3	6	41	16	54
6	6.6	4	42	10	46
7	3.1	6	46	21	59
8	5.3	6	40	18	56
9	2.4	6	45	30	67
10[b]	7.0	24	28	16	54
11	6.4	12	45	10	46
12	5.0	6	40	11	48

[a] Ar^1X (first addition) = 1-iodo-4-*n*-alkoxybenzene. Ar^2X (second addition) = 1-bromo-3-fluoro-4-*n*-alkoxybenzene. Reaction conditions of first addition: 1.2–1.9 mL of THF, 1.02–1.08 mmol of 2-methyl-3-butyn-2-ol, and 4.0–4.5 mol % $PdCl_2(PPh_3)_2$ per mmol of Ar^1X; 2 mol of NEt_3 per mol of 2-methyl-3-butyn-2-ol; CuI:PD:PPh_3 = 3.7:1:5.3; reflux. Reaction conditions of second addition: 1 mmol of Ar^2X and 0.30–0.83 mL of THF per mmol of Ar^1X; 2.6–3.3 mol of KHO and 20 mol % TBAH per mol of 2-methyl-3-butyn-2-ol of first addition; reflux. [b] CuI:Pd:PPh_3 = 4.0:1:14.7.

Results

Synthesis of 1,2-Bis(3-fluoro-4-*n*-alkoxyphenyl)-acetylenes and 1-(3-Fluoro-4-*n*-alkoxyphenyl)-2-(4-*n*-alkoxyphenyl)acetylenes. The 1,2-bis(3-fluoro-4-*n*-alkoxyphenyl)acetylenes were prepared by the first route

Scheme II. One-Pot, Phase-Transfer Pd(0)/Cu(I)-Catalyzed Synthesis of 1,2-Bis[3-fluoro-4-*n*-alkoxyphenyl]acetylenes and 1-(3-Fluoro-4-*n*-alkoxyphenyl)-2-(4-*n*-alkoxyphenyl)-acetylenes

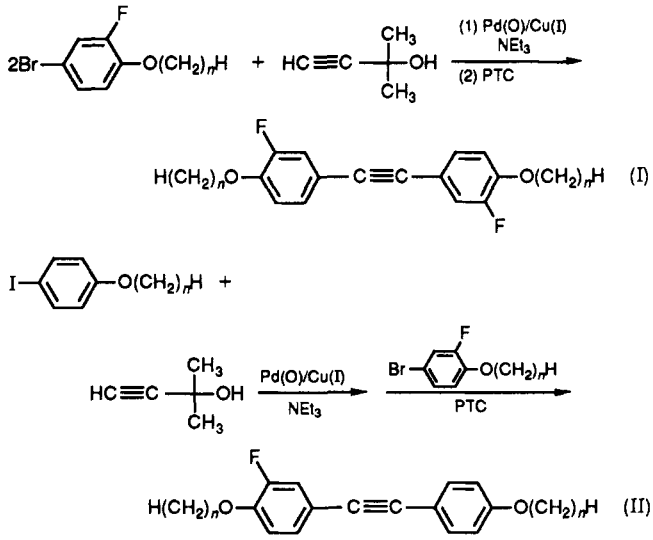

outlined in Scheme II. We previously reported that symmetrical 1,2-bis(4-alkoxyaryl)acetylenes could be prepared from the corresponding aryl iodide and 2-methyl-3-butyn-2-ol under solid–liquid PTC conditions in which both coupling and deprotection can take place simultaneously.[1] However, we have recently found that the less reactive aryl bromides fail to react under these conditions and instead require that the first coupling step takes place by deprotonation with an organic base.[15] Therefore, the symmetrical 1,2-bis(3-fluoro-4-*n*-alkoxyphenyl)acetylenes were prepared by first refluxing 2 equiv of aryl bromide with 1 equiv of 2-methyl-3-butyn-2-ol in THF for at least 6 h, using triethylamine as base. Deprotection of the resulting carbinol derivative followed by coupling with the second equivalent of aryl bromide was achieved by continued refluxing after adding solid KOH and TBAH.

The results of the phase-transfer Pd(0)/Cu(I)-catalyzed coupling reactions using 1-bromo-3-fluoro-4-*n*-alkoxybenzenes are presented in Table I. The 25–62% yields obtained are similar to those achieved by using aryl iodides.[1] Also included in Table I are the cube root of the yield, since this represents the average yield obtained from each of the three steps. In addition, if traditional procedures were used, 63–85% isolated yields would therefore have to be obtained from each of the three steps to obtain the same overall yield from this one-pot procedure.

The results of the phase-transfer Pd(0)/Cu(I)-catalyzed coupling reactions to form asymmetric 1-(3-fluoro-4-*n*-alkoxyphenyl)acetylenes by the second route outlined in Scheme II are summarized in Table II. In this case, the second aryl halide is not added to the reaction mixture until the first aryl halide has reacted completely. The first aryl halide coupling is generally over within 2–3 h, although we have allowed at least one extra hour of reaction time to ensure complete conversion. However, a much longer time was required when a PPh_3/PD ratio of 14.7 rather than 5.3 was used. Triphenylphosphine is added to reduce $PdCl_2(PPh_3)_2$ to $Pd(PPh_3)_4$. Because $Pd(PPh_3)_4$ is in equilibrium with the tris and bis derivatives[16]

$$Pd(PPh_3)_4 \rightleftharpoons PPh_3 + Pd(PPh_3)_3 \rightleftharpoons 2PPh_3 + Pd(PPh_3)_2$$

(15) Pugh, C.; Percec, V., to be published.

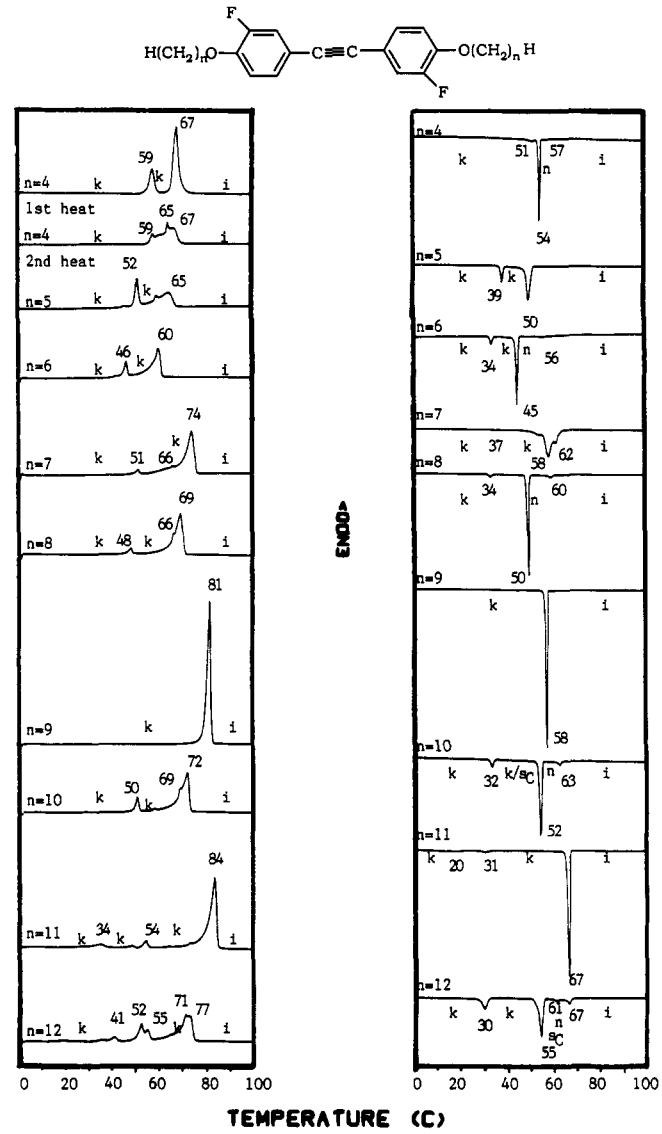

Figure 1. DSC heating and cooling scans of symmetrically difluorinated 1,2-bis(3-fluoro-4-*n*-alkoxyphenyl)acetylenes.

and because Pd(0) requires two vacant coordination sites to undergo oxidative addition with the aryl halide, it is understandable that the reaction rate decreases with increasing triphenylphosphine relative to Pd.

The isolated yields of the 1-(3-fluoro-4-*n*-alkoxyphenyl)-2-(4-*n*-alkoxyphenyl)acetylenes ranged from 10 to 30%, corresponding to an averaged 46–67% yield from each of the three steps. However, as we have demonstrated previously,[1] it is the deprotection step that limits the reaction rate.

Thermal Characterization. The DSC traces observed on heating and cooling in the 1,2-bis(3-fluoro-4-*n*-alkoxyphenyl)acetylenes are presented in Figure 1. Their complete thermal transitions are summarized in Table III. The crystallization and isotropic to nematic transition temperatures of this symmetrically difluorinated series are depressed relative to the analogous nonfluorinated 1,2-bis(4-*n*-alkoxyphenyl)acetylenes.[3] Because the liquid-crystalline transitions are depressed more than the crystalline transitions, only monotropic nematic mesophases are observed in the even members of this series.

(16) Collman, J. P.; Hegedus, L. S. *Principles and Applications of Organotransition Metal Chemistry*; University Science Books: Mill Valley, CA, 1980; p 58.

Table III. Thermal Transitions and Thermodynamic Parameters of 1,2-Bis(3-fluoro-4-*n*-alkoxyphenyl)acetylenes[a]

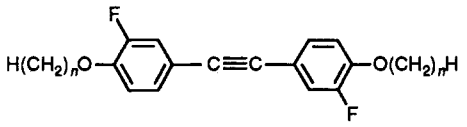

n	phase transitions, °C (corresponding enthalpy changes, kcal/mol)
4	k 58.6 k 64.9 k 67.1 (5.47)[b] i 57.4 n 54.5 k 51.4 (5.06)[b]
5	k 45.9 k 51.6 k 59.7 k 65.2 (7.65)[b] i i 50.1 (5.43) k 38.7 (1.53) k
6	k 46.2 (1.79) k 60.0 (5.70) i i 56.0 (0.25) n 45.0 (5.46) k 33.6 (0.71) k
7	k 51.2 k 66.1 k 74.5 (11.41)[b] i i 62.2 k 58.4 (10.5)[b] k 37.1 (0.17) k 27.7 (0.08) k
8	k 47.7 (0.54) k 69.3 (9.23) i i 59.8 (0.41) n 49.6 (8.56) k 33.6 (0.38) k
9	k 81.3 (14.4) i i 57.9 (13.7) k
10	k 50.9 (1.82) k 69.5 k 72.5 (12.0)[b] i i 62.9 (0.65) n 54.1 (9.27) s_C/k 33.5 (1.06) k
11	k 34.5 (1.34) k 48.5 (0.54) k 54.3 (0.77) k 83.6 (15.9) i i 67.2 (15.3) k 30.7 k 19.5 (1.42)[b] k i[c] 77.6 n 75.6 s_C 71.6 k
12	k 18.8 (0.26) k 35.4 k 41.0 (0.85)[b] k 52.4 k 55.0 (4.77)[b] 65.4 k 71.4 k 73.1 (9.63)[b] i i 66.7 n 61.4 (1.43)[b] s_C 54.6 (7.16) k 30.1 (2.94) k

[a] k = crystalline, s = smectic, n = nematic, i = isotropic melt; first line of data obtained on heating, second line on cooling. [b] Overlapped with previous transition(s). [c] From microscope, -3 °C/min.

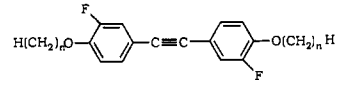

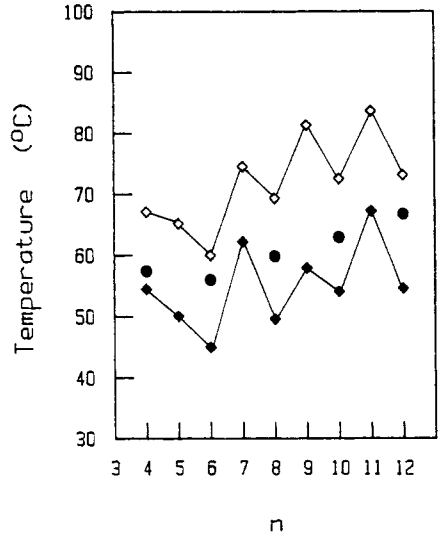

Figure 2. Melting (◇), crystallization (◆) and isotropic–nematic (●) transition temperatures of symmetrically difluorinated 1,2-bis[3-fluoro-4-*n*-alkoxyphenyl]acetylenes as a function of *n*.

All odd members of this series are crystalline molecules with only a virtual nematic mesophase. As shown in Figure 2, the crystalline ↔ nematic and nematic ↔ isotropic transitions display opposite odd–even alternation as a function of the length of the *n*-alkoxy substituents. This is the same unusual relationship observed in the analogous nonfluorinated 1,2-bis(4-*n*-alkoxyphenyl)acetylenes,[3] except that the nematic mesophases of the hydrogen analogues are more stable and enantiotropic for both odd and even members of the series. In both cases, the opposite odd–even alternation results in larger mesophase temperature windows for the even members of the series than for the odd members. The n = 7–12 homologous 1-(4-*n*-alkylphenyl)-2-(4-cyanophenyl)acetylenes[17–20] also present opposite odd–even alternation, with the even members displaying monotropic nematic mesophases and the odd members displaying enantiotropic nematic mesophases.

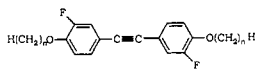

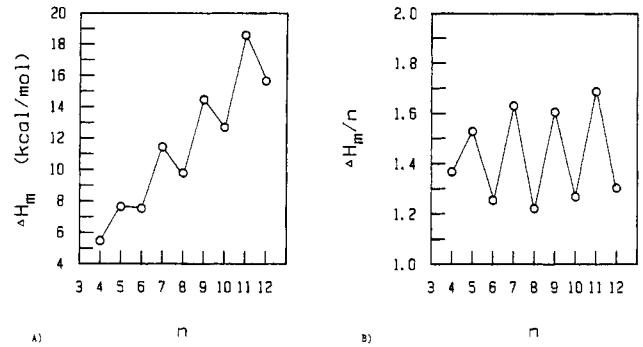

Figure 3. Change in enthalpy (A) and change in enthalpy per methylenic unit (B) of the complete melting transition(s) on heating 1,2-bis[3-fluoro-4-*n*-alkoxyphenyl]acetylenes as a function of *n*.

A second trend observed in Figure 2 is that the transition temperatures generally increase as n increases, indicating that order within the molecules is due primarily to ordering of the alkoxy side chains rather than to packing of the mesogens. This is also demonstrated by the fact that the total change in enthalpy upon melting increases as n increases, albeit in an odd–even alternation (Figure 3A). The change in enthalpy per methylenic unit also increases slightly as n increases (Figure 3B). As with the melting temperature, the corresponding ΔH and $\Delta H/n$ are lower in the even members of the series.

The ability of 1,2-bis[3-fluoro-4-(*n*-butyloxy)phenyl]-acetylene to pack into a three-dimensional crystal is evidently disfavored both by having short alkoxy chains and by having an even number of methylenic units in those chains. As shown in Figure 1, 1,2-bis[3-fluoro-4-(*n*-butyloxy)phenyl]acetylene crystallizes much better from solution (first heat) than from the melt (second heat). Therefore, the melting transition of melt-crystallized material is very broad and multistep in nature. 1,2-Bis-[3-fluoro-4-(*n*-pentyloxy)phenyl]acetylene also presents a broad, multistep melting transition of relatively low enthalpy. The shape of the melting transition is similar for the rest of the series. However, it becomes sharper as n increases to a single peak at n = 9 and thereafter broadens into multistep peaks.

As with the nonfluorinated diphenylacetylenes with long *n*-alkoxy chains, the 1,2-bis(3-fluoro-4-*n*-alkoxyphenyl)-acetylenes with n = 10–12 display monotropic s_C mesophases upon cooling from the nematic phase. This is seen clearly by DSC only for the n = 12 derivative. However, the nematic to s*C* transition is seen by polarized optical

(17) Gray, G. W.; Mosley, A. *Mol. Cryst. Liq. Cryst.* **1976**, *37*, 213.
(18) Cox, R. J.; Clecak, N. J. *Mol. Cryst. Liq. Cryst.* **1976**, *37*, 241.
(19) Cox, R. J.; Gaskill, R. C.; Johnson, J. F.; Clecak, N. J. *Thermochim. Acta* **1977**, *18*, 37.
(20) Adomenas, P.; Butkus, V.; Daugvila, J.; Dienyte, J.; Girdziunaite, D. In *Advances in Liquid Crystalline Research and Applications*; Bata, L., Ed.; Pergamon Press: Oxford, 1980; Vol. II, p 1029.

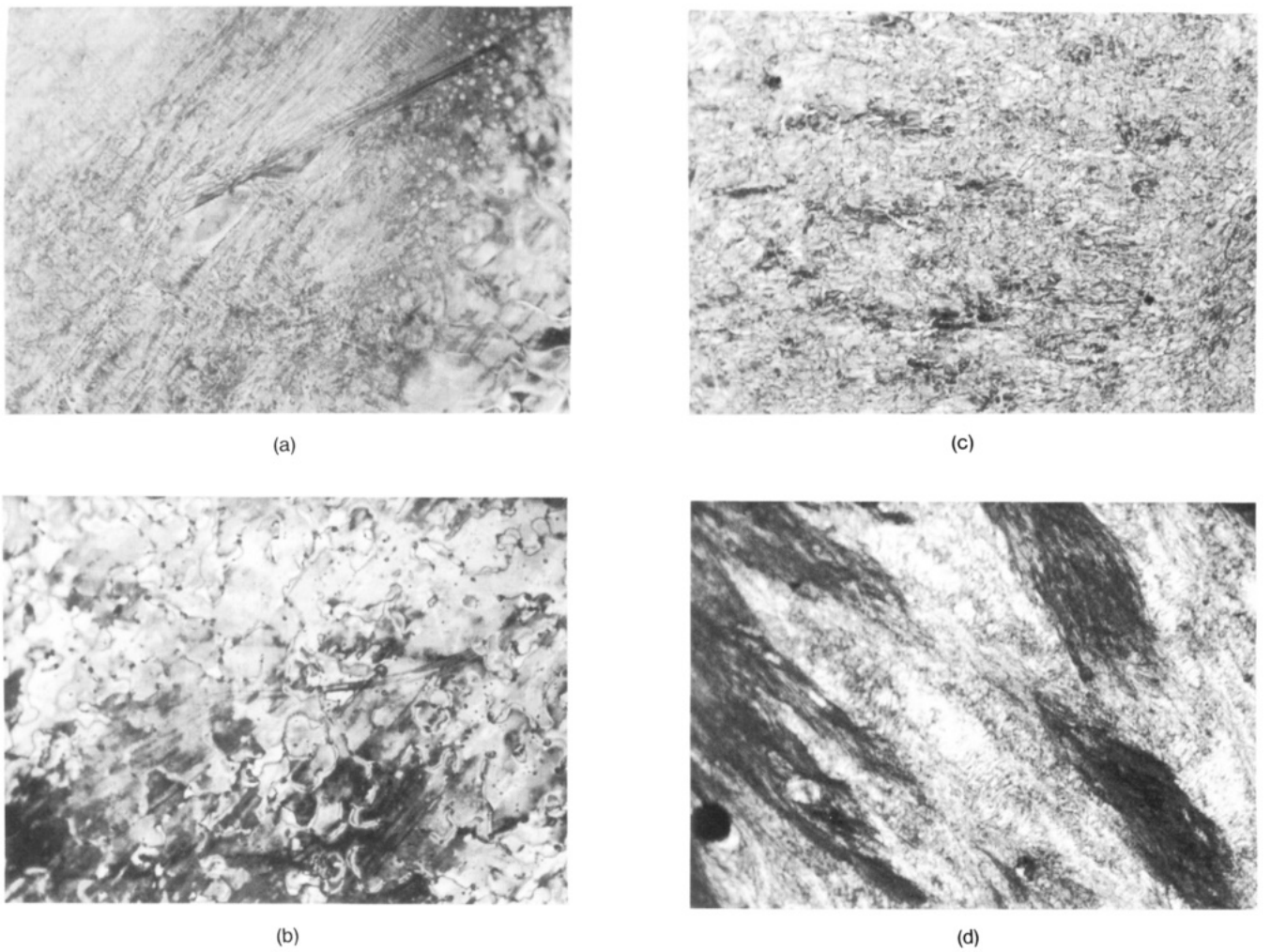

Figure 4. Polarized optical micrographs (100×) of the textures exhibited by 1,2-bis[3-fluoro-4-(*n*-decyloxy)phenyl]acetylene: (A) 63.7 °C, s_C and nematic mesophases forming simultaneously by cooling from 74.1 °C at 3 °C/min; (B) 62.2 °C, nematic mesophase formed by cooling from 84 °C at 10 °C/min; (C) 65.9 °C, s_C mesophase formed by cooling from 74.1 °C at 3° C/min, observed on heating; (D) 50.0 °C, polymorphic k/s_C phases formed by cooling from 84 °C at 10 °C/min.

microscopy in all three compounds. For example, when cooling 1,2-bis[3-fluoro-(*n*-decyloxy)phenyl]acetylene on the microscope at 10 °C/min, the s_C and crystalline phases form simultaneously, resulting in a polymorphic solid. However, if this compound is cooled at 3 °C/min, the nematic and s_C phases form simultaneously, with the nematic portion immediately transforming to an s_C phase. This is shown in Figure 4A, with the s_C phase forming on the left side of the optical micrograph, and nematic droplets forming on the right side. Figure 4B–D shows the pure nematic, pure s_C, and polymorphic crystalline/s_C phases, respectively. The nematic to s_C to crystalline transitions of 1,2-bis[3-fluoro-4-(*n*-undecyloxy)phenyl]-acetylene are rapidly observed in succession on the microscope at both −3 and −10 °C/min with each phase undergoing a complete transition to the next ordered phase. The crystalline phases of both the n = 11 and 12 derivatives are homogeneous.

The DSC traces observed on heating and cooling the 1-(3-fluoro-4-*n*-alkoxyphenyl)-2-(4-*n*-alkoxyphenyl)-acetylenes with n = 5–12 are presented in Figure 5. Their complete thermal transitions are summarized in Table IV. 1-[3-Fluoro-4-(pentyloxy)phenyl]-2-[4-(pentyloxy)-phenyl]acetylene displays two sharp melting/crystallization transitions of relatively low enthalpy and supercooling. However, due to the stabilization of liquid-crystalline phase in 1,2-bis(4-alkoxyphenyl)acetylenes by asymmetry,[3] those compounds with n = 6–10 display stable enantiotropic

Table IV. Thermal Transitions and Thermodynamic Parameters of 1-(3-Fluoro-4-*n*-alkoxyphenyl)-2-(4-*n*-alkoxyphenyl)-acetylenes[a]

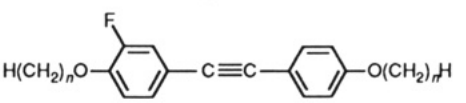

n	phase transitions, °C (corresponding enthalpy changes, kcal/mol)
5	k 68.7 (2.60) k 85.8 (6.34) i i 78.1 (5.98) k 62.1 (2.51) k
6	k 61.2 (.86) k 74.8 (5.51) n 78.6 (0.23) i i 76.4 (0.36) n 66.4 (5.71) k 18.7 (0.52) k
7	k 60.1 (6.59) s 68.9 (2.98) n 76.3 (0.34) i i 73.8 (0.38) n 64.2 (3.12) s 35.6 (6.80) k
8	k 60.7 k 62.9 (6.99)[b] s 68.2 (2.99) n 82.0 i i 79.2 (0.74) n 63.3 (3.16) s 52.9 (3.60) k 47.3 (5.54) k
9	k 75.0 (12.6) n 80.2 (0.41) i i 77.8 (0.56) n 65.1 (.36) s_C 59.9 (11.9) k
10	k 51.4 k 66.5 (10.8)[b] n 82.4 (0.86) i i 80.1 (0.82) n 66.6 (0.34) s_C 46.2 (8.25) k 36.4 (1.15) k 28.3 (1.38) k
11	k 84.2 (19.2) i i 75.6 n 74.1 (1.81)[b] s_C 69.8 k
12	k 83.0 (18.9) i i 80.2 (2.41) n→s_C 69.3 (13.6) k

[a] k = crystalline, s = smectic, n = nematic, i = isotropic melt; first line of data obtained on heating, second line on cooling. [b] Overlapped with previous transition.

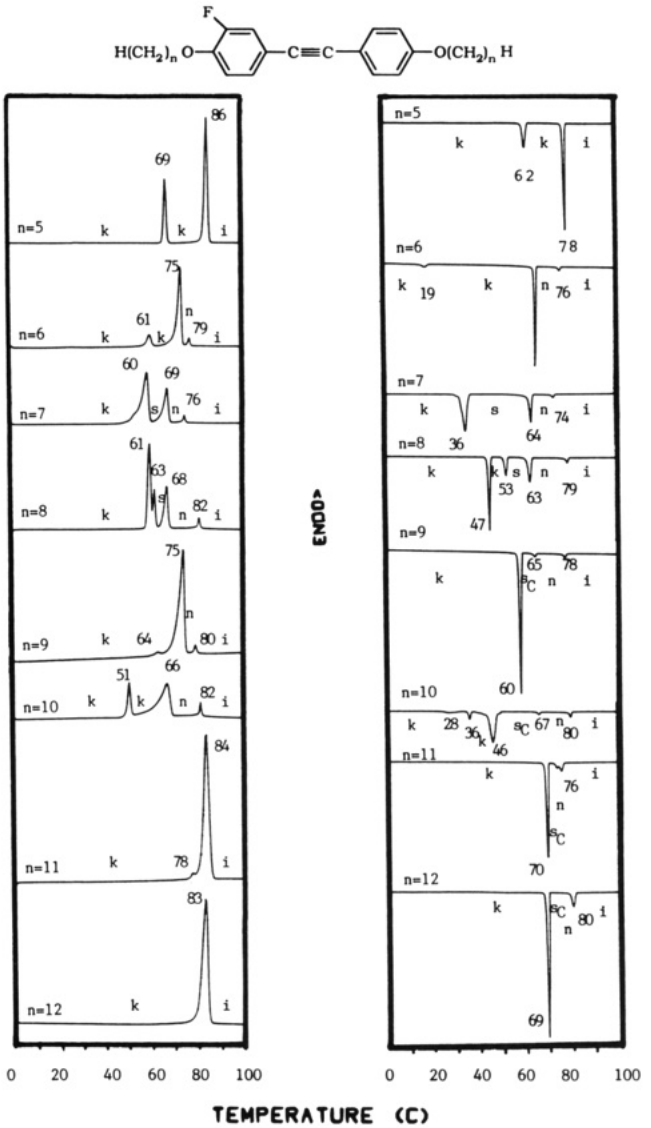

Figure 5. DSC heating and cooling scans of asymmetric monofluorinated 1-(3-fluoro-4-*n*-alkoxyphenyl)-2-(4-*n*-alkoxyphenyl)acetylenes.

nematic mesophases. The nematic mesophases of the derivatives with n = 11, 12 are monotropic.

The DSC heating traces of this asymmetric monofluorinated series with n = 6–10 strongly resemble those of the symmetric, nonfluorinated 1,2-bis(4-*n*-alkoxyphenyl)acetylenes, except that all transition temperatures are depressed. In addition, there is evidently less kinetic control of the various transitions since polymorphism is not observed by optical microscopy. All transitions are sharp and well defined on both heating and cooling. The crystalline versus higher ordered smectic transitions can therefore by assigned with more certainty. In addition to an enantiotropic nematic mesophase, those compounds with n = 7 and 8 also display an enantiotropic smectic mesophase with a mosaic texture. This again demonstrates that a smectic mesophase must be involved in the polymorphism of the 1,2-bis(4-*n*-alkoxyphenyl)acetylenes with n = 4–8.

The nematic mesophase of 1-[3-fluoro-4-(nonyloxy)phenyl]-2-[4-(nonyloxy)phenyl]acetylene is monotropic. In addition, it forms a monotropic smectic mesophase. However, in contrast to the higher ordered smectic mesophase of 1,2-bis[4-(nonyloxy)phenyl]acetylene which exhibits a large mosaic texture, this monofluorinated analogue presents an s_C mesophase. The higher homologues with n = 10–12 also present monotropic s_C mesophases. 1-[3-Fluoro-4-(decyloxy)phenyl]-2-[4-(decyloxy)phenyl]acetylene has both a wide s_C temperature window (21 °C) and a fairly wide (13 °C) nematic window on cooling. In contrast, the monotropic nematic window is very small in the n = 11, 12 homologues. As shown in Figure 6, the s_C phase actually forms in the nematic droplets of 1-[3-fluoro-4-(dodecyloxy)phenyl]-2-(4-(dodecyloxy)phenyl)acetylene.

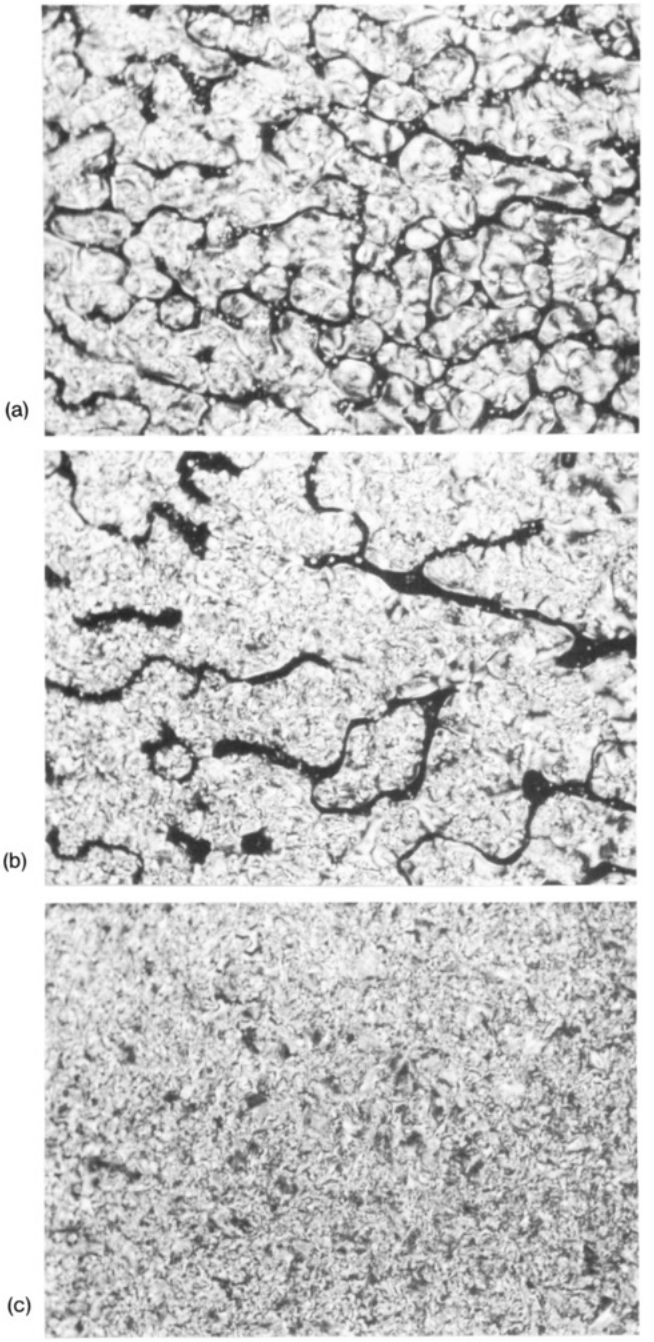

Figure 6. Polarized optical micrographs (100×) of the textures exhibited by 1-[3-fluoro-4-(*n*-dodecyloxy)phenyl]-2-[4-(*n*-dodecyloxy)phenyl]acetylene on cooling from the isotropic state: (A) 80.6 °C, nematic droplets; (B) 80.6 °C, a few seconds later, s_C mesophase within nematic droplets; (C) 79.0 °C, s_C mesophase.

The various transitions of the 1-(3-fluoro-4-*n*-alkoxyphenyl)-2-(4-*n*-alkoxyphenyl)acetylenes are plotted in Figure 7 as a function of the number of methylenic units in the *n*-alkoxy side chains. Although the melting/crystalline transitions are more eratic than in the 1,2-bis(3-fluoro-4-*n*-alkoxyphenyl)acetylene series, there is again a

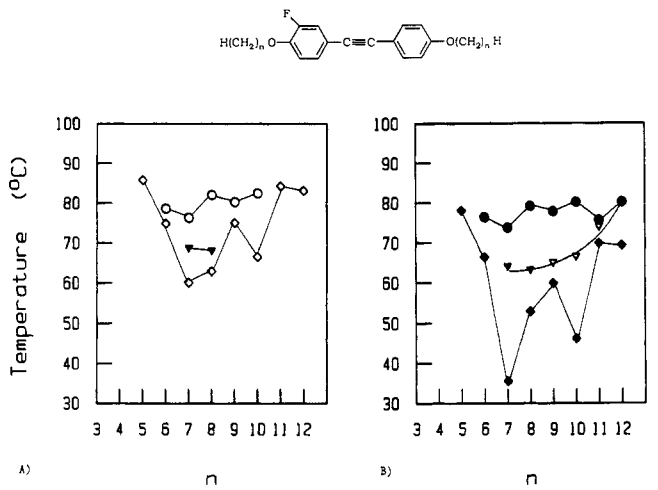

Figure 7. Melting (◇), n → i (○) and s → n (▼) observed (A) on heating 1-(3-fluoro-4-*n*-alkoxyphenyl)-2-(4-*n*-alkoxyphenyl)-acetylenes, and crystallization (◆), i → n (●), n → s (▼) and n → s_C (▽) observed (B) on cooling.

general increase in the transition temperatures with increasing *n* and opposite odd–even alternation of melting/crystallization versus isotropization.

Discussion

The DSC traces of 1,2-bis[3-fluoro-4-(heptyloxy)-phenyl]acetylene, 1,2-bis[3-fluoro-4-(nonyloxy)phenyl]-acetylene, 1-bis[3-fluoro-4-(heptyloxy)phenyl]-2-[4-(heptyloxy)phenyl]acetylene, and 1-[3-fluoro-4-(nonyloxy)-phenyl]2-[4-(nonyloxy)phenyl]acetylene are plotted in Figure 8, along with their hydrogen and methyl analogues. In all cases, isotropization is depressed more than crystallization by both methyl and fluorine substitution. This is especially obvious in the symmetrically disubstituted derivatives, which do not exhibit smectic or nematic mesophases and are only crystalline when $n = 7, 9$. However, when either a methyl or fluorine substituent is introduced in only one of the aromatic rings, enantiotropic nematic mesophases are also observed. 1-[3-Fluoro-4-heptyloxy)-phenyl]-2-[4-(heptyloxy)phenyl]acetylene also exhibits an enantiotropic smectic mesophase, and 1-[3-fluoro-4-(nonyloxy)phenyl]-2-[4-(nonyloxy)phenyl]acetylene also exhibits a monotropic s_C mesophase. Therefore, lateral fluoride substitution has less of a destabilization effect on the liquid-crystalline mesophases of 1,2-bis(4-*n*-alkoxyphenyl)acetylenes than does lateral methyl substitution.

In contrast, the crystalline phase of fluorinated terphenyls is generally destabilized more than the liquid-crystalline phases.[7,9] Fluorinated phenyl benzoates show both types of behavior.[7] That is, if the phenyl ring is 2,3-difluorinated, then the liquid-crystalline phase is destabilized more. However, if the carboxylate ring is 2,3-difluorinated, then the crystalline phase is more strongly depressed. We have previously demonstrated that there is a competition between stabilization of liquid-crystalline phases by extension of the mesogenic length and destabilization by lateral substitution.[3,4] The former effect evidently dominates in the fluorinated terphenyls. We expect that liquid-crystalline destabilization by lateral substitution in the diphenylacetylenes would eventually be compensated for by extension of the mesogenic length. Although the nematic mesophase of 1,4-bis[2-(4-(heptyloxy)phenyl)ethynyl]benzene was more destabilized by lateral methyl substitution than was the crystalline phase,[4] lateral fluorine substitution in the extended compound might result in less nematic destabilization since fluorine has less of a destabilizing effect than does methyl. This

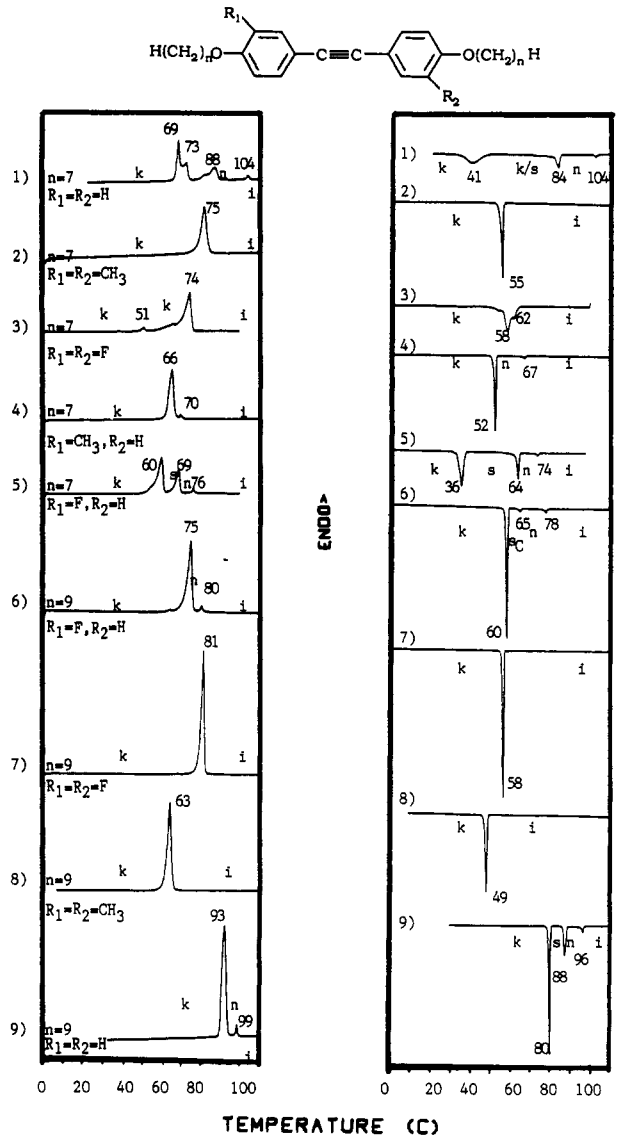

Figure 8. DSC heating and cooling scans of symmetric and assymmetric 1,2-bis(4-*n*-alkoxyphenyl)acetylenes ($n = 7, 9$) with either fluorine or methyl branches in the mesogen and their unbranched analogues.

seems to be confirmed by the fact that the nematic mesophase of 1-[2,3-difluoro-4-(ethyloxy)phenyl]-2-[4-(pentyloxy)phenyl]acetylene is destabilized more than the crystalline phase relative to its nonfluorinated analogue, whereas the opposite is true if the mesogen is extended by one cyclohexyl ring.[7]

Acknowledgment. Financial support from the U.S. Army Research Office is gratefully acknowledged.

Registry No. $H_3CC(OH)(CH_3)C{\equiv}CH$, 115-19-5; $PdCl_2(PPh_3)_2$, 13965-03-2; CuI, 7681-65-4; PPh_3, 603-35-0; 1-bromo-3-fluoro-4-(butyloxy)benzene, 54509-63-6; 1-bromo-3-fluoro-4-(pentyloxy)benzene, 127326-78-7; 1-bromo-3-fluoro-4-(hexyloxy)benzene, 54509-62-5; 1-bromo-3-fluoro-4-(heptyloxy)benzene, 56308-72-6; 1-bromo-3-fluoro-4-(octyloxy)benzene, 119259-26-6; 1-bromo-3-fluoro-4-(nonyloxy)benzene, 127326-79-8; 1-bromo-3-fluoro-4-(decyloxy)benzene, 119828-40-9; 1-bromo-3-fluoro-4-(undecyloxy)benzene, 127326-80-1; 1-bromo-3-fluoro-4-(dodecyloxy)-benzene, 122265-74-1; 1-iodo-4-(pentyloxy)benzene, 116223-55-3; 1-iodo-4-(hexyloxy)benzene, 85557-94-4; 1-iodo-4-(heptyloxy)-benzene, 116223-56-4; 1-iodo-4-(octyloxy)benzene, 96693-06-0; 1-iodo-4-(nonyloxy)benzene, 116223-57-5; 1-iodo-4-(decyloxy)-benzene, 93144-80-0; 1-iodo-4-(undecyloxy)benzene, 116223-58-6; 1-iodo-4-(dodecyloxy)benzene, 116223-59-7; 1,2-bis[3-fluoro-4-(butyloxy)phenyl]acetylene, 129921-32-0; 1,2-bis[3-fluoro-4-

(pentyloxy)phenyl]acetylene, 129921-33-1; 1,2-bis[3-fluoro-4-(hexyloxy)phenyl]acetylene, 129921-34-2; 1,2-bis[3-fluoro-4-(heptyloxy)phenyl]acetylene, 129921-35-3; 1,2-bis[3-fluoro-4-(octyloxy)phenyl]acetylene, 129921-36-4; 1,2-bis[3-fluoro-4-(nonyloxy)phenyl]acetylene, 129921-37-5; 1,2-bis[3-fluoro-4-(decyloxy)phenyl]acetylene, 129921-38-6; 1,2-bis[3-fluoro-4-(decyloxy)phenyl]acetylene, 129921-39-7; 1,2-bis[3-fluoro-4-(dodecyloxy)phenyl]acetylene, 129921-40-0; 1-[3-fluoro-4-(pentyloxy)phenyl]-2-[4-(pentyloxy)phenyl]acetylene, 129921-41-1; 1-[3-fluoro-4-(hexyloxy)phenyl]-2-[4-(hexyloxy)phenyl]acetylene, 129921-42-2; 1-[3-fluoro-4-(heptyloxy)phenyl]-2-[4-(heptyloxy)phenyl]acetylene, 129921-43-3; 1-[3-fluoro-4-(octyloxy)phenyl]-2-[4-(octyloxy)phenyl]acetylene, 129921-44-4; 1-[3-fluoro-4-(nonyloxy)phenyl]-2-[4-(nonyloxy)phenyl]acetylene, 129921-45-5; 1-[3-fluoro-4-(decyloxy)phenyl]-2-[4-(decyloxy)phenyl]acetylene, 129942-72-9; 1-[3-fluoro-4-(undecyloxy)phenyl]-2-[4-(undecyloxy)phenyl]acetylene, 129942-73-0; 1-[3-fluoro-4-(dodecyloxy)phenyl]-2-[4-(dodecyloxy)phenyl]acetylene, 129942-74-1.

Characterization of the $Bi_{1.6}Pb_{0.4}Sr_2Ca_2Cu_3O_y$ Superconductor by X-ray Diffraction, Low-Field Microwave Absorption, and Electron Spin Resonance

Stephane Cuvier, Micky Puri,* John Bear, and Larry Kevan*

Department of Chemistry and the Texas Center for Superconductivity, University of Houston, Houston, Texas 77204-5641

Received May 30, 1990. Revised Manuscript Received September 19, 1990

X-ray diffraction (XRD) and low-field microwave absorption (LFMA) have been measured for a series of $Bi_{1.6}Ph_{0.4}Sr_2Ca_2Cu_3O_y$ superconducting samples prepared at different sintering temperatures that display zero resistance between 50 and 98 K. Multiphase formation is observed in all samples. XRD results suggest that the fraction of the high-transition temperature (T_c) phase denoted as 2223 grows with increasing sintering time and temperature compared to the low-T_c phase denoted as 2212, although the 2212 phase always predominates. Simultaneously, several impurity phases also increase. The 2223 phase and 2210 phase seem to be formed by the disproportionation of the 2212 phase. The incorporation of Pb in the lattice accelerates this disproportionation process. LFMA signals reveal the presence of two superconducting phases with T_c close to 75 and 115 K. The intensity of the microwave absorption due to the low T_c phase is 3–6 times higher than that of the high T_c phase. This suggests that between the two transition temperatures, the magnetic shielding of the high T_c phase is weakened by penetration of the magnetic flux in the bulk material through the low T_c phase, when the latter becomes nonsuperconducting above its transition temperature. No electron spin resonance signal has been detected for this superconducting system above or below T_c, which indicates the lack of paramagnetic impurity phases.

Introduction

It is generally accepted that the two high-temperature superconducting phases in the BiSrCaCuO system have nominal compositions of $Bi_2Sr_2CaCu_2O_y$ (2212) with T_c near 80 K and $Bi_2Sr_2Ca_2Cu_3O_y$ (2223) with T_c near 110 K.[1-5] The $Bi_2Sr_2CuO_y$ phase (2201) is a low-temperature superconductor with a $T_c \sim 10$ K. The 2212 phase formation is the most facile, and hence it always is the dominant species. It is more difficult to prepare the 2201 and 2223 phases. It has been shown by Cava et al.[6] that Pb substitution for Bi promotes the formation of the 2223 phase when the correct stoichiometric amounts of starting materials are used. A 10–30 mol % Pb substitution for Bi is reported to be the optimum ratio for 2223 phase formation.[7-11] Furthermore, lead substitution also appears to affect the speed of reaction so that similar material can be produced in a shorter time.[11,12]

Other methods reported to accelerate the formation of the 2223 phase are sintering under reduced oxygen partial pressure,[9] modification of starting composition,[9,13] careful control of sintering temperature,[7,8,14,15] antimony[16] and/or vanadium[17] substitution for bismuth, and partial replacement of oxygen by fluorine.[18] A reduction in oxygen content to enhance T_c of the 2212 phase has been accomplished by quenching,[19,20] argon, nitrogen, or hydrogen treatment, and thermal cycling.[15,21] Even without Pb substitution, a T_c above 95 K has been reported.[20,27]

* To whom correspondence should be addressed at the Department of Chemistry.

(1) Michel, C.; Hervieu, M.; Borel, M. M.; Grandin, A.; Deslandes, F.; Provost, J.; Raveau, B. *Z. Phys. B* **1987**, *68*, 421.
(2) Maeda, H.; Tanaka, Y.; Fukutomi, M.; Asano, T. *Jpn. J. Appl. Phys.* **1988**, *27*, 209.
(3) McGuire, T. R.; Shivashankav, S. A.; La Placa, S. J.; Chandrashekhar, G. V.; Boehme, R. F.; Shaw, T. M.; Yee, D. S.; Shafer, M. W.; Cuomo, J. J. *J. Appl. Phys.* **1988**, *64*, 5792.
(4) Dabrowski, B.; Richards, D. R.; Hinks, D. G.; Hannon, R. H.; Peng, W.; Lee, H.; Genis, A. P.; Melim, V. I.; Kimball, C. W. *Physica C* **1989**, *160*, 281.
(5) Torardi, C. C.; Subramanian, M. A.; Calabrese, J. C.; Gopalakrishnan, J.; McCarron, E. M.; Morrissey, K. J.; Askew, T. R.; Flippen, R. B.; Chowdry, U.; Sleight, A. W. *Phys. Rev. B* **1988**, *38*, 225.
(6) Cava, R. J.; Batlogg, B.; Sunshine, S. A.; Siegrist, T.; Fleming, R. M.; Babe, R.; Shneemeyer, L. F.; Murphy, D. W.; van Dover, R. B.; Gallagher, P. K.; Glarum, S. H.; Nakahara, S.; Farrow, R. C.; Krajewski, J. J.; Zahurak, S. M.; Waszcak, J. V.; Marshall, J. H.; Marsh, P.; Rupp Jr., L. W.; Peck, W. F.; Rietman, E. A. *Physica C* **1988**, *158*, 247.
(7) Oota, A.; Kirihigashi, A.; Sasaki, Y. Y.; Ohba, K. *Jpn. J. Appl. Phys.* **1988**, *27*, 2050.
(8) Koyama, S.; Endo, U.; Kawai, T. *Jpn. J. Appl. Phys.* **1988**, *27*, 1861.
(9) Endo, U.; Koyama, S.; Kawai, T. *Jpn. J. Appl. Phys.* **1989**, *28*, 190.
(10) Liu, H. K.; Dou, S. X.; Savvides, N.; Zhou, J. P.; Tan, M. X.; Bourdillon, A. J.; Kviz, M.; Sorrell, C. C. *Physica C* **1989**, *157*, 93.
(11) Flower, M. E.; Presland, M. R.; Gilberd, P.; Buckley, R. G. *Physica C* **1990**, *165*, 161.
(12) Mohan Ram, R. A.; Kobiela, P. S.; Kirk, W. P.; Clearfield, A. *J. Solid State Chem.* **1989**, *83*, 214.
(13) Sasakura, H.; Minamigawa, Nakahigachi, K.; Kogachi, M.; Nakanishi, S.; Fukuoka, N.; Yoshikawa, M.; Noguchi, S.; Okuda, K.; Yanase, A. *Jpn. J. Appl. Phys.* **1989**, *28*, 1163.

0897-4756/91/2803-0115$02.50/0